

Ferroelectricity in epitaxial Y-doped HfO₂ thin film integrated on Si substrate

K. Lee, T. Y. Lee, S. M. Yang, D. H. Lee, J. Park, and S. C. Chae

Citation: *Appl. Phys. Lett.* **112**, 202901 (2018); doi: 10.1063/1.5020688

View online: <https://doi.org/10.1063/1.5020688>

View Table of Contents: <http://aip.scitation.org/toc/apl/112/20>

Published by the [American Institute of Physics](#)

Articles you may be interested in

[Tiered deposition of sub-5 nm ferroelectric Hf_{1-x}Zr_xO₂ films on metal and semiconductor substrates](#)

Applied Physics Letters **112**, 192901 (2018); 10.1063/1.5027516

[Evolution of ferroelectric HfO₂ in ultrathin region down to 3 nm](#)

Applied Physics Letters **112**, 102902 (2018); 10.1063/1.5017094

[Non-linear variation of domain period under electric field in demagnetized CoFeB/MgO stacks with perpendicular easy axis](#)

Applied Physics Letters **112**, 202402 (2018); 10.1063/1.5035487

[Effect of film thickness on the ferroelectric and dielectric properties of low-temperature \(400 °C\) Hf_{0.5}Zr_{0.5}O₂ films](#)

Applied Physics Letters **112**, 172902 (2018); 10.1063/1.5026715

[Interplay between ferroelectric and resistive switching in doped crystalline HfO₂](#)

Journal of Applied Physics **123**, 134102 (2018); 10.1063/1.5015985

[Large ferroelectric polarization of TiN/Hf_{0.5}Zr_{0.5}O₂/TiN capacitors due to stress-induced crystallization at low thermal budget](#)

Applied Physics Letters **111**, 242901 (2017); 10.1063/1.4995619

PHYSICS TODAY

WHITEPAPERS

MANAGER'S GUIDE

Accelerate R&D with
Multiphysics Simulation

READ NOW

PRESENTED BY

 COMSOL

Ferroelectricity in epitaxial Y-doped HfO₂ thin film integrated on Si substrate

K. Lee,¹ T. Y. Lee,¹ S. M. Yang,² D. H. Lee,^{3,4} J. Park,^{3,4} and S. C. Chae^{1,a)}

¹Department of Physics Education, Seoul National University, Seoul 08826, South Korea

²Department of Physics, Sookmyung Women's University, Seoul 04310, South Korea

³School of Chemical and Biological Engineering, Institute of Chemical Processes, Seoul National University, Seoul 08826, South Korea

⁴Center for Nanoparticle Research, Institute for Basic Science (IBS), Seoul 08826, South Korea

(Received 26 December 2017; accepted 21 March 2018; published online 14 May 2018)

We report on the ferroelectricity of a Y-doped HfO₂ thin film epitaxially grown on Si substrate, with an yttria-stabilized zirconia buffer layer pre-deposited on the substrate. Piezoresponse force microscopy results show the ferroelectric domain pattern, implying the existence of ferroelectricity in the epitaxial HfO₂ film. The epitaxially stabilized HfO₂ film in the form of a metal-ferroelectric-insulator-semiconductor structure exhibits ferroelectric hysteresis with a clear ferroelectric switching current in polarization-voltage measurements. The HfO₂ thin film also demonstrates ferroelectric retention comparable to that of current perovskite-based metal-ferroelectric-insulator-semiconductor structures. *Published by AIP Publishing.* <https://doi.org/10.1063/1.5020688>

Since the unprecedented discovery of ferroelectricity in HfO₂, a well-known high-*k* material,¹ non-centrosymmetric orthorhombic HfO₂ has attracted attention as a possible replacement for ternary perovskite materials in ferroelectric memory devices.^{2–6} In the early 2000s, the critical thickness for ferroelectricity in Pb-based perovskite materials restricted the scalability of ferroelectric memory down to 130 nm in complementary metal oxide semiconductor (CMOS) processing;^{7,8} however, ferroelectricity has been observed in orthorhombic HfO₂ films thinner than 10 nm, further suggesting its suitability as an alternative to perovskite materials in ferroelectric random access memory (FeRAM). In particular, the removal of the restriction in scalability enhances the possibility of CMOS-compatible processing of ferroelectric HfO₂ and industrial applications for ferroelectric memory devices.

The complexity of the device structure, including traditional switching and memory cells, introduces a further limitation to device fabrication. To reduce this complexity, a single transistor-based ferroelectric random access memory (1T-FeRAM) device has been proposed based on nonvolatile channel conductivity modulated by the ferroelectric field effect.⁹ The complexity of the switching and memory cells, particularly the three-dimensional capacitor structure, can be reduced using the different non-volatile channel conductivities induced by the ferroelectric field effect. In contrast to a single transistor-single capacitor structure (1T-1C), which uses a memory cell with opposing ferroelectric polarity as binary information, the scalability of the 1T-FeRAM structure can be best exploited in a metal-ferroelectric HfO₂-insulator-semiconductor structure.

Realization of HfO₂-based 1T-FeRAM requires understanding of the underlying mechanism governing the ferroelectric field effect and of the gate channel conductivity and its ferroelectric origin. In this respect, epitaxial ferroelectric HfO₂ on Si is a suitable platform for further study. Most work on the origin of ferroelectricity in HfO₂ has concentrated on the crystal structure of the HfO₂ film; however,

chemical disorder or mechanical strain may be considered as control parameters for device operation. For example, oxygen vacancy movement can be attributed to the wake-up effect, where the saturation polarization value increases during external voltage cycling.¹⁰ The epitaxial HfO₂ thin film with less structural disorders like grain boundary will enlarge the understanding of ferroelectricity observed in the polycrystalline HfO₂ thin film.^{11–13}

In this letter, we report the ferroelectric behavior of a Y-doped HfO₂ (YHO) thin film epitaxially stabilized on Si substrate with an yttria-stabilized zirconia (YSZ) buffer layer. YSZ has been used as a buffer layer to stabilize various oxide materials epitaxially on Si substrates, due to its chemical stability on the Si substrate and adequate lattice mismatch with YHO.^{14,15} Conventional polarization-voltage (P-V) measurements, piezoresponse force microscopy (PFM), and X-ray diffraction were used to investigate ferroelectricity in a non-centrosymmetric ferroelectric HfO₂ based metal-ferroelectric-insulator-semiconductor (MFIS) structure. The strong hysteresis observed in the P-V was attributed to ferroelectricity in the ultra-thin YHO film.

Epitaxial ferroelectric YHO thin films were prepared by pulsed laser deposition (PLD) on a YSZ-buffered Si (001) substrate (YHO/YSZ/Si (001)). The Si ($\leq 0.005 \Omega\cdot\text{cm}$, p-type) substrate was etched using 1:10 HF buffer oxide etchant to remove the SiO₂ layer. A KrF excimer laser with a wavelength of 248 nm, an energy density of 2 J/cm², and a frequency of 3 Hz was used. The YSZ film was deposited at 750 °C under oxygen at a partial pressure of 4×10^{-4} Torr. After YSZ film deposition, the YHO film was deposited at 700 °C and 150 mTorr. For the electrical contact, Pt was deposited by e-beam evaporation to a thickness of 30 nm, using a shadow mask of dimensions $45 \times 45 \mu\text{m}^2$. To investigate the crystal structure of the YHO film, X-ray diffraction θ - 2θ , φ scan, and reciprocal space mapping measurements were conducted using a high resolution X-ray diffractometer (D8-Discover; Bruker, Billerica, MA, USA). Transmission electron microscopy (TEM) was conducted (JEM-2100F; JEOL, Tokyo, Japan) to confirm structural disorder during

^{a)}Electronic mail: scchae@snu.ac.kr

the high temperature deposition. The ferroelectric properties of the YHO film were confirmed with local polarization switching via piezoresponse force microscopy (PFM) (Cypher; Asylum Research, Santa Barbara, CA, USA), ferroelectric hysteresis using a P-V sweep, ferroelectric retention property measurements (TF Analyzer 3000; aixACCT Systems GmbH, Aachen, Germany), and a capacitance–voltage (C-V) sweep (Impedance Analyzer E4990A; Keysight, Santa Barbara, CA, USA).

Highly (001) oriented YHO thin films were grown coherently on a YSZ-buffered Si (001) substrate. Figure 1(a) shows the X-ray θ - 2θ scan patterns of the YHO thin film grown on the YSZ-buffered Si (001) substrate. The single YSZ film of the same thickness showed no peak associated with (00 l) diffraction due to the low diffraction intensity.¹⁶ Various HfO₂ crystal structures have been suggested as the origin of ferroelectricity, and the metastable orthorhombic phase of HfO₂ has been the primary focus of discussions.¹⁻⁶ The peak around 35° which corresponds to 0.513 nm can be considered as a mixture of (001) and (010) orthorhombic HfO₂ phases with similar lattice constants along the b- and c-axes. Considering the ferroelectric behavior discussed

below, the (002) peak corresponds to the out-of-plane polarization direction of the orthorhombic YHO thin film while the (020) peak corresponds to the in-plane-direction polarization.¹⁵ The X-ray θ - 2θ scans show no evidence of secondary YHO phases, exhibiting only the out-of-plane directional orthorhombic HfO₂ (020)/(002) peak.

The in-plane epitaxy of the YHO films was investigated using an X-ray ϕ scan and reciprocal space mapping. Figure 1(b) shows the X-ray ϕ scan patterns measured at the YHO (202) (top) and Si (202) (bottom) reflections. The four distinct diffraction patterns separated by 90° indicate that the film has the four-fold symmetry of the (001)-oriented YHO film with in-plane epitaxy coherent with the in-plane crystallinity of the Si substrate. In addition, as shown in Fig. 1(c), the reciprocal space mapping around the Si (113) peak shows the coincidence with the orthorhombic HfO₂ (113) peak with relaxation of in-plane lattice parameters, $a = 0.518$ nm and $b = 0.514$ nm, respectively. The in-plane lattice constants were estimated from the X-ray θ - 2θ of Si (202), data not shown, as well as HfO₂ (202) peaks. The X-ray θ - 2θ , ϕ scans, and reciprocal space mapping imply that the epitaxial orthorhombic HfO₂ film on Si with out-of-plane polarization was fabricated.

Further transmission electron microscopy (TEM) investigation indicated that coherent HfO₂ thin film growth was achieved globally with few secondary structural phases. Figure 1(d) shows a cross sectional TEM image of the HfO₂/YSZ/Si (001) structure and indicates that the YHO thin films were crystallized epitaxially on the YSZ buffer layer. In order to clear the atomic stacking of the orthorhombic HfO₂ film, we conducted the Fourier transform of the dashed rectangular region of the TEM image in Fig. 1(d) and rebuilt the stacking image by the inverse Fourier transform (IFT) as shown in Figs. 1(e) and 1(f), respectively. Figure 1(f) was obtained from the diffraction patterns indicated by the yellow circles in Fig. 1(e). Clear atomic stripe patterns were observed with few fractures along different structural orientations or grain boundaries and significant interdiffusion between layers. No definite grain boundary structures except for the edge dislocations noted by dashed red circle in Fig. 1(f) were observed in the rebuilt IFT image. The intermediate amorphous layer between the Si substrate and the YSZ buffer layer in Fig. 1(d) is an SiO₂ layer. Even though the pristine SiO₂ layer was removed by etching, an amorphous SiO₂ layer with a thickness of ~ 2 nm can exist without limiting the epitaxial growth of other layers.¹⁶

To investigate the microscopic ferroelectric response under an external bias, local ferroelectric polarization switching under tip-biasing during PFM scanning was conducted. Figure 2(a) shows the surface morphology of the YHO film obtained by atomic force microscopy. The film exhibited a very flat surface without distinct grain structures with a root mean square roughness of 0.3 nm. Figures 2(b) and 2(c) show out-of-plane PFM amplitude and phase images after +10 V ($2 \times 2 \mu\text{m}^2$) and -10 V ($1 \times 1 \mu\text{m}^2$) were applied through the tip, respectively. The typical box pattern of written domains was observed in both amplitude and phase images. The inset of Fig. 2(c) shows the line profile of the piezoresponse indicated in Fig. 2(c). The as-grown film has almost no piezoresponse signal due to the randomly

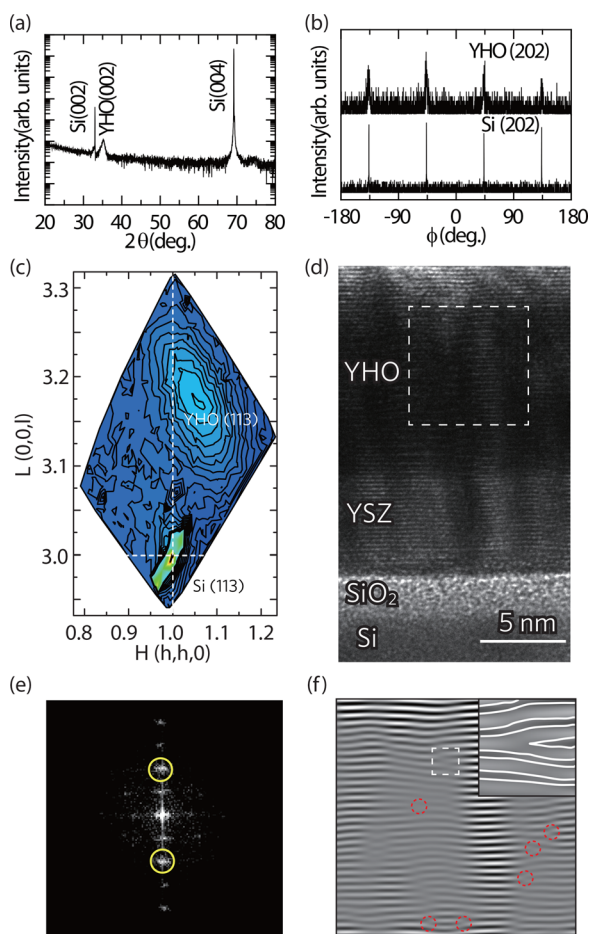


FIG. 1. (a) X-ray θ - 2θ diffraction pattern of the epitaxial Y-doped HfO₂ (YHO) thin film on the yttria-stabilized zirconia (YSZ)-buffered Si (001) substrate. (b) X-ray ϕ scans of YHO (202) (top) and Si (202) (bottom). (c) Reciprocal space mapping around the Si (113) peak. (d) Transmission electron microscopy (TEM) image of the epitaxial YHO thin film on the YSZ-buffered Si (001) substrate. (e) The Fourier transform image of the dashed rectangle in (d). (f) The inverse Fourier transform image of (e) with spots in yellow circles. The inset shows the enlarged area denoted by the dashed rectangle.

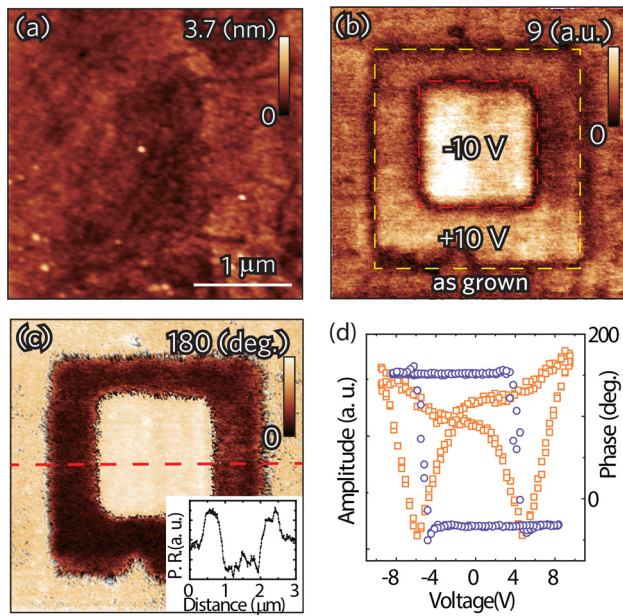


FIG. 2. Local piezo response of the YHO film on the YSZ-buffered Si (001) substrate. (a) Atomic force microscopy image with a RMS roughness of 0.3 nm. (b) Piezoresponse force microscopy (PFM) amplitude image ($3 \mu\text{m} \times 3 \mu\text{m}$). (c) PFM phase image ($3 \mu\text{m} \times 3 \mu\text{m}$). The inset shows the piezo response line profile [red line in (c)] after +10 V and -10 V domain-switching process. (d) Piezoresponse spectroscopy amplitude (empty orange square) and phase (empty purple circle).

ordered polarizations, while the written region scanned with opposite tip bias exhibited two distinct piezoresponse values, corresponding to upward and downward polarization. Figure 2(d) shows local piezoresponse spectroscopy measurements on the YHO film. Typical hysteresis loops were observed with transient 180° phase shifts at -6 V and $+5 \text{ V}$, corresponding to the ferroelectric phase changes. These results indicate that our YHO film has reversible local polarization of ferroelectricity.¹⁷

The P-V hysteresis measurements were conducted to further investigate the macroscopic ferroelectric properties of the YHO film. Figure 3(a) shows the transient current dependence of the external voltage of the YHO thin film. The polarization value was estimated by integrating the switching current against the applied voltage. As shown in Fig. 3(b), a clear P-V hysteresis loop was observed along the out-of-plane direction, corresponding to the polarization direction. A difference in the coercive field measured by PFM and conventional P-V hysteresis was observed; the frequency dependence of the coercive voltage can induce different coercive fields between piezoresponse spectroscopy (DC bias sweep) and P-V (2 kHz ac sweep) loops.¹⁸ A clear switching current was observed when the applied voltage amplitude was larger than 10 V. However, as the applied voltage was increased, a non-linear leakage current due to the Schottky contact was observed, deforming the well-saturated hysteresis loop. Unsaturated hysteresis loops usually occur on MFIS structures.^{19,20} While many of these unsaturated hysteresis loops show P-V curves without a concave region (in which ferroelectric switching currents are negligible),²¹ our YHO film shows clear switching current peaks, indicated by the mark in Fig. 3(a). A remnant

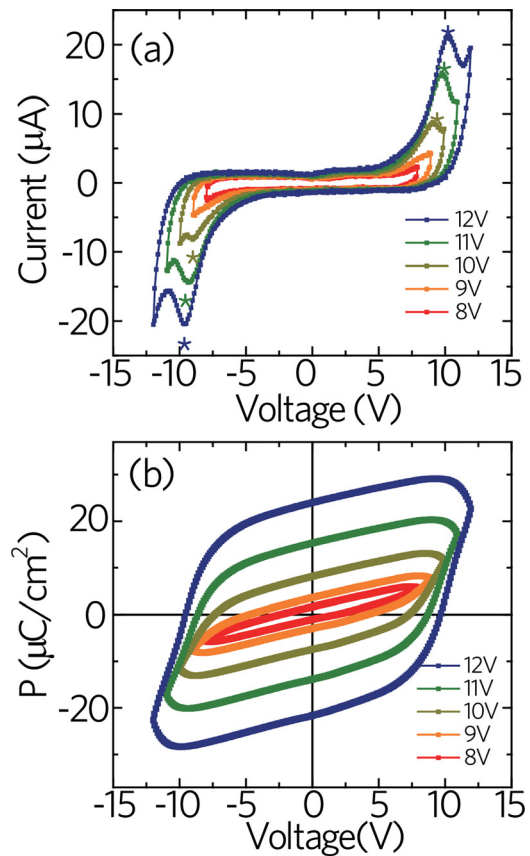


FIG. 3. Polarization-voltage measurements for the epitaxial YHO film on the YSZ-buffered Si (001) substrate with the voltage width and frequency of 8–12 V and 2 kHz, respectively. (a) Transient response of ferroelectric switching current and (b) polarization.

polarization of around $20 \mu\text{C}/\text{cm}^2$ was observed when the applied voltage amplitude was 12 V. Experimental and theoretical expected remnant polarization values are around $40 \mu\text{C}/\text{cm}^2$ for YHO,^{22–24} and the mixture of out-of-plane directional YHO (010) and in-plane (001) phases or depletion of the Si can be attributed to the reduced polarization value.^{19,21}

The flat band voltage difference in the C-V characteristics, i.e., the memory window for MFIS devices, can be induced by either polarization of the ferroelectric film or bound charges near the interface due to remnant polarization of ferroelectrics.⁹ Figure 4 shows a C-V sweep of the YHO film at 1 MHz. Counterclockwise directional hysteresis in the C-V measurements was observed for our HfO_2 -based MFIS on a p-type Si substrate, with a memory window in the 6 V sweep of around 0.7 V. The counterclockwise hysteresis indicates charge accumulation and dissipation of injected carriers with ferroelectric polarization of the YHO film.^{19,25} As the amplitude of the sweep voltage increased, the positive direction sweep shifts leftwards, while the negative direction sweep remains almost the same as shown in the inset of Fig. 4, indicating that the memory window of this sample was induced by hole carrier injection. The capacitances of YHO/YSZ/SiO₂ and YSZ/SiO₂ were measured as 12.4 and 15.9 pF, respectively, from the capacitance of the YHO/YSZ/SiO₂ and YSZ/SiO₂ in the saturated charge accumulation region. Considering the series configuration of YHO/

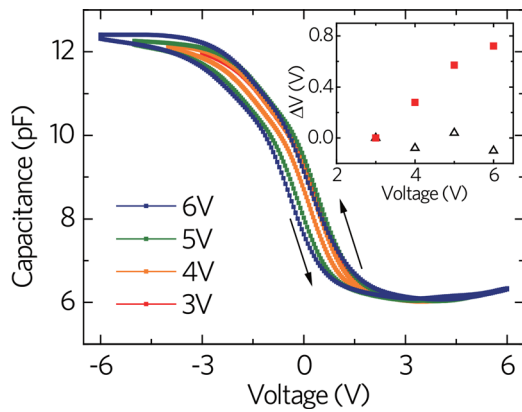


FIG. 4. Capacitance-voltage (C-V) characteristics of the YHO film on YSZ-buffered Si (001) at 1 MHz with 3–6 V DC amplitude sweep. The arrows in the figure indicate the voltage sweep directions. The inset shows the sweep voltage bias dependence of threshold voltage. The solid rectangles and empty triangles show the positive and negative polarity dependences, respectively.

YSZ/SiO₂, the capacitance of the YHO layer was estimated to be 56.3 pF and the effective dielectric constants of YHO and YSZ/SiO₂ to be 37.7 and 6.21, respectively. From the experimental coercive voltage for the heterostructure, ~ 9.5 V, the coercive field of the YHO film was estimated to be ~ 1.74 MV/cm for the voltage sweep up to 12 V. The estimated coercive field value is well-matched with the coercive field values of ferroelectric HfO₂ films.^{1–6,23}

The ferroelectric retention loss was investigated using a writing (reading) voltage of 12 V and a pulse width of 125 μ s. Figure 5(a) shows the retention properties of ferroelectric polarization for the YHO MFIS structure at room temperature. Slow relaxation of ferroelectric polarization with a stretched exponential decay, $P(t)/P_0 = \exp(-(t/t_0)^\beta)$, was observed. Stretched exponential behavior with $\beta < 1$ can be considered as random walk-based partial polarization switching arising from the gate leakage current or the depolarization field.^{26,27} The β values for the positive and negative applied voltages were estimated to be 0.26 and 0.35, respectively. These values are comparable with random walk-type processes in poly-crystalline Pb(Zr_xTi_{1-x})O₃ (0.24–0.68).²⁶ For retention, the t_0 values were about 9.6×10^6 s and 4.3×10^5 s for positive and negative voltages, respectively. Both polarization directions are expected to remain stable even after 10 days, comparable to other current MFIS

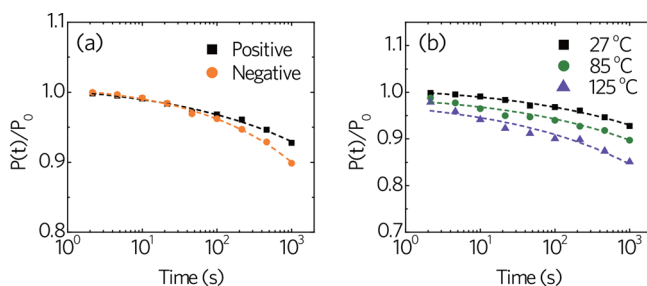


FIG. 5. (a) Retention of ferroelectric polarization of the epitaxial YHO film on the YSZ-buffered Si (001) substrate polled positively and negatively at room temperature. The dashed lines in the experimental results indicate the stretched exponential decay of ferroelectric polarizations of opposite poles. (b) High temperature retentions of the YHO film at 85 °C and 125 °C compared with the case of room temperature.

structures.^{28–30} The initial retention loss is mainly affected by the leakage current caused by the random walk process. A higher leakage current was observed under negative versus positive voltages, as shown in Fig. 3(a), and this causes the difference in retention time for each polarization direction. Furthermore, we checked the high temperature retention loss of remnant polarization polled positively at 85 °C and 125 °C for the circumstance in the real device operation. Figure 5(b) shows that the t_0 values for 85 °C and 125 °C were 4.6×10^6 s and 1.5×10^6 s, respectively, which are comparable with the retention at room temperature. The high coercive field for polarization switching with an order of 1 MV/cm can be responsible for the low decrease in remnant polarization during the retention measurement.^{11–13}

In conclusion, we have demonstrated epitaxial YHO integrated on a Si platform. X-ray diffraction analysis demonstrated that epitaxial crystallization through YSZ was successfully achieved by PLD. The clear PFM and ferroelectric P-E hysteresis confirmed ferroelectricity along the out-of-plane direction in the HfO₂ film. The epitaxial YHO film exhibited retention properties comparable with current perovskite material-based ferroelectric memory devices.

This work was supported by the MOTIE (Ministry of Trade, Industry and Energy) (No. 10080657) and KRSC (Korea Semiconductor Research Consortium) support program for the development of future semiconductor devices. Part of this study was performed using facilities at the IBS Center for Correlated Electron Systems, Seoul National University. S.M.Y. was also supported by a National Research Foundation of Korea (NRF) grant funded by the Korean Government (MSIP) (No. NRF-2017R1C1B2010258). TEM experiments were supported by No. IBS-R006-D1.

¹T. Böschke, J. Müller, D. Bräuhäus, U. Schröder, and U. Böttger, *Appl. Phys. Lett.* **99**, 102903 (2011).

²M. H. Park, Y. H. Lee, H. J. Kim, Y. J. Kim, T. Moon, K. D. Kim, J. Müller, A. Kersch, U. Schroeder, T. Mikolajick, and C. S. Hwang, *Adv. Mater.* **27**, 1811 (2015).

³X. Sang, E. D. Grimley, T. Schenk, U. Schroeder, and J. M. LeBeau, *Appl. Phys. Lett.* **106**, 162905 (2015).

⁴T. Shimizu, K. Katayama, T. Kiguchi, A. Akama, T. J. Konno, and H. Funakubo, *Appl. Phys. Lett.* **107**, 032910 (2015).

⁵S. Starschich, D. Griesche, T. Schneller, R. Waser, and U. Böttger, *Appl. Phys. Lett.* **104**, 202903 (2014).

⁶J. Müller, T. S. Böschke, U. Schröder, S. Mueller, D. Bräuhäus, U. Böttger, L. Frey, and T. Mikolajick, *Nano Lett.* **12**, 4318 (2012).

⁷L. Shaoping, A. E. Jeffery, M. V. James, M. F. Christopher, E. N. Robert, and L. E. Cross, *Jpn. J. Appl. Phys.* **36**, 5169 (1997).

⁸T. S. Moise, S. R. Summerfelt, H. McAdams, S. Aggarwal, K. R. Udayakumar, F. G. Celii, J. S. Martin, G. Xing, L. Hall, K. J. Taylor, T. Hurd, J. Rodriguez, K. Remack, M. D. Khan, K. Boku, G. Stacey, M. Yao, M. G. Albrecht, E. Zielinski, M. Thakre, S. Kuchimanchi, A. Thomas, B. McKee, J. Rickes, A. Wang, J. Grace, J. Fong, D. Lee, C. Pietrzyk, R. Lanham, S. R. Gilbert, D. Taylor, J. Amano, R. Bailey, F. Chu, G. Fox, S. Sun, and T. Davenport, in *International Electron Devices Meeting. Technical Digest* (2002), p. 535.

⁹W. Shu-Yau, *IEEE Trans. Electron Devices* **21**, 499 (1974).

¹⁰S. Starschich, S. Menzel, and U. Böttger, *Appl. Phys. Lett.* **108**, 032903 (2016).

¹¹J. Müller, T. S. Böschke, U. Schroeder, R. Hoffmann, T. Mikolajick, and L. Frey, *IEEE Electron Device Lett.* **33**, 185 (2012).

¹²T. S. B. J. Müller, S. Müller, E. Yurchuk, P. Polakowski, J. Paul, D. Martin, T. Schenk, K. Khullar, A. Kersch, W. Weinreich, S. Riedel, K. Seidel, A. Kumar, T. M. Arruda, S. V. Kalinin, T. Schlösser, R. Böschke,

- R. V. Bentum, U. Schröder, and T. Mikolajick, in *International Electron Devices Meeting* (2013), p. 10. 8. 1.
- ¹³E. Yurchuk, J. Muller, R. Hoffmann, J. Paul, D. Martin, R. Boschke, T. Schlosser, S. Muller, S. Slesazeck, R. v. Bentum, M. Trentzsch, U. Schroder, and T. Mikolajick, in *4th IEEE International Memory Workshop (IMW)* (2012), p. 1.
- ¹⁴D. Fork, D. Fenner, G. Connell, J. M. Phillips, and T. Geballe, *Appl. Phys. Lett.* **57**, 1137 (1990).
- ¹⁵K. Katayama, T. Shimizu, O. Sakata, T. Shiraishi, S. Nakamura, T. Kiguchi, A. Akama, T. J. Konno, H. Uchida, and H. Funakubo, *J. Appl. Phys.* **119**, 134101 (2016).
- ¹⁶S. Jun, Y. S. Kim, J. Lee, and Y. W. Kim, *Appl. Phys. Lett.* **78**, 2542 (2001).
- ¹⁷C. Dubourdieu, J. Bruley, T. M. Arruda, A. Posadas, J. Jordan-Sweet, M. M. Frank, E. Cartier, D. J. Frank, S. V. Kalinin, A. A. Demkov, and V. Narayanan, *Nat. Nanotechnol.* **8**, 748 (2013).
- ¹⁸D. Viehland and Y.-H. Chen, *J. Appl. Phys.* **88**, 6696 (2000).
- ¹⁹F. Zhang, Y.-C. Perng, J. H. Choi, T. Wu, T.-K. Chung, G. P. Carman, C. Locke, S. Thomas, S. E. Sadow, and J. P. Chang, *J. Appl. Phys.* **109**, 124109 (2011).
- ²⁰S. H. Lim, A. C. Rastogi, and S. B. Desu, *J. Appl. Phys.* **96**, 5673 (2004).
- ²¹J. F. Scott, *J. Phys.: Condens. Matter* **20**, 021001 (2008).
- ²²S. Clima, D. J. Wouters, C. Adelman, T. Schenk, U. Schroeder, M. Jurczak, and G. Pourtois, *Appl. Phys. Lett.* **104**, 092906 (2014).
- ²³T. Shimizu, K. Katayama, T. Kiguchi, A. Akama, T. J. Konno, O. Sakata, and H. Funakubo, *Sci. Rep.* **6**, 32931 (2016).
- ²⁴U. Schroeder, E. Yurchuk, J. Müller, D. Martin, T. Schenk, P. Polakowski, C. Adelman, M. Popovici, S. V. Kalinin, and T. Mikolajick, *Jpn. J. Appl. Phys.* **53**, 08LE02 (2014).
- ²⁵S. Kundu, D. Maurya, M. Clavel, Y. Zhou, N. N. Halder, M. K. Hudait, P. Banerji, and S. Priya, *Sci. Rep.* **5**, 8494 (2015).
- ²⁶A. Gruverman, H. Tokumoto, A. S. Prakash, S. Aggarwal, B. Yang, M. Wuttig, R. Ramesh, O. Auciello, and T. Venkatesan, *Appl. Phys. Lett.* **71**, 3492 (1997).
- ²⁷A. Morelli, S. Venkatesan, G. Palasantzas, B. J. Kooi, and J. T. M. D. Hosson, *J. Appl. Phys.* **102**, 084103 (2007).
- ²⁸B.-E. Park, K. Takahashi, and H. Ishiwara, *Appl. Phys. Lett.* **85**, 4448 (2004).
- ²⁹T. Li, S. T. Hsu, B. D. Ulrich, and D. R. Evans, *Appl. Phys. Lett.* **86**, 123513 (2005).
- ³⁰M. H. Tang, Z. H. Sun, Y. C. Zhou, Y. Sugiyama, and H. Ishiwara, *Appl. Phys. Lett.* **94**, 212907 (2009).